

Study and Realization of a Prototype Octocopter System with PID Controller

Saidi Hemza^a and Djebri Boualem^b

^aDept. of Engg., Mohamed Boudiaf University of Sci. and Tech., Oran, Algeria

Corresponding Author, Email: hamzaing2008@yahoo.fr

^bLaboratory City, Architecture and Heritage Polytechnique School of Architecture and Town planning, Algeria

Email: h.saidi@univ-chlef.dz

ABSTRACT:

In this work, the mechanical and electrical components are designed and realised for an octocopter. The designed system dynamic model is supported with Euler-Lagrangian model and Newton-Euler model respectively for the rotational and transnational movements of the drone. The prototype octocopter is also equipped with a proportional integral derivative controller to feedback both location and respond to the external environment.

KEYWORDS:

Octocopter; Aerodynamics; System dynamics; Brushless DC electric motor; Proportional integral derivative controller

CITATION:

S. Hemza and D. Boualem. 2018. Study and Realization of a Prototype Octocopter System with PID Controller, *Int. J. Vehicle Structures & Systems*, 10(4), 273-277. doi:10.4273/ijvss.10.4.09.

NOMENCLATURE:

$A (\vec{X}, \vec{Y}, \vec{Z})$	Fixed terrestrial reference
$B (\vec{x}, \vec{y}, \vec{z})$	Movable marker fixed at the center of the octocopter
F_i	Lift force created by each rotor [N]
g	Gravity acceleration [m/s^2]
Φ, θ, ψ	Angle of roll, pitch and yaw [rad]
ωm	Rotational speed of each rotor [rad/s]
I_x, I_y, I_z	Inertia along the axis $\vec{x}, \vec{y}, \vec{z}$ [kgm^2]
J_{rot}	Total inertia around propeller axis [$kg m^2$]
J	Symmetrical dimension inertia matrix
F_t	Drag force along the axes (x, y, z) [N]
M_y, M_x, M_z	Moment of lift along the axis $\vec{x}, \vec{y}, \vec{z}$
Ω	Angular velocity [rad/s]
M_xg, M_yg	Gyroscopic torque along the axis \vec{x}, \vec{y}
$\ddot{X}, \ddot{Y}, \ddot{Z}$	Linear accelerations at fixed terrestrial reference [m/s^2]
$\ddot{\Phi}, \ddot{\theta}, \ddot{\Psi}$	Angular accelerations at fixed terrestrial reference [rad/s^2]
T, V	Kinetic and potential energy [J]
iL	Lagrangian
K_p, K_i, K_d	Proportional, integral and derivative gain of PID controller
v_x^b, v_y^b, v_z^b	Linear velocities in the fixed ref. [m/s]
v_x^m, v_y^m, v_z^m	Linear velocities in the movable coordinate system [m/s]
v	Translation speed [m/s]
m	Total mass of octocopter [kg]
i	Number of rotor [1:8]

1. Introduction

In order to design a flight controller for a drone, we must first deeply understand its movements, including its system dynamics. Indeed, the comprehension of the latter is necessary for the design of the controller on one

hand and to ensure simulations of the air vehicle's behaviour if they are closer to the reality on the other hand. The octocopter is characterized as the most complex flying system influenced by several factors such as aerodynamic effects, gravity, gyroscopic effects, friction and moment of inertia. Using a quadcopter model [1], we have succeeded to produce an octocopter model. As shown in Fig. 1, by dividing the force of a rotor on an arm of the quadrirotor, two symmetric forces similar in comparison with the arm of the quadrirotor can be found. This is done for each arm of the quadrirotor to obtain an octocopter model.

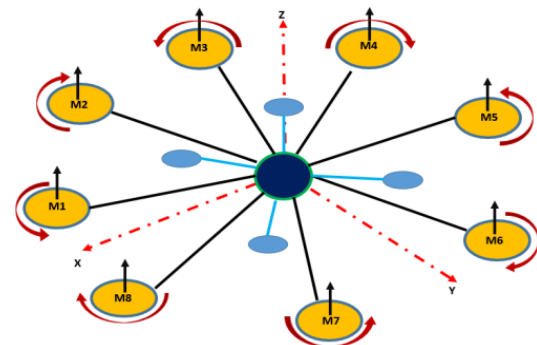


Fig. 1: Basis of octocopter model from quadcopter principle

2. Dynamic model of the octocopter

The hypotheses and assumptions towards design of the system dynamic model for the octocopter are as follows,

- 1) The structure of the octocopter is assumed to be rigid and symmetric, which implies that the inertia matrix will be assumed to be diagonal.
- 2) The rotors are supposed to be rigid, so that we can neglect the effect of their deformation during rotation.

- 3) The center of the mass coincides with the origin of the reference point linked to the structure.
- 4) The lift forces and the motor speeds are proportional to the squares of the rotational speed of the rotors, which is an approximation very close to the aerodynamic behaviour.

Cartesian co-ordinate system allows designating a rotation by the Euler angles. To obtain the mathematical model representing the behaviour of the octocopter, we use two reference points: one fixed reference point linked to the operator A ($\vec{X}, \vec{Y}, \vec{Z}$) and another movable B ($\vec{x}, \vec{y}, \vec{z}$) linked to the octocopter. The advantage of the fixed reference mark of the operator is to evaluate the trajectory and the movement of the moving frame. For the transport between the two landmarks the rotations are generally used. First around the axis \vec{z} , then around the axis \vec{y} and finally around the axis \vec{x} . These rotations are expressed by rotation matrices R (\vec{x}, Φ), R (\vec{y}, θ) and R (\vec{z}, Ψ). The passage of the fixed mark A ($\vec{X}, \vec{Y}, \vec{Z}$) to the mark B ($\vec{x}, \vec{y}, \vec{z}$) is made using,

$$R = Rot_x(\Psi) \times Rot_y\theta \times Rot_x(\Phi)$$

$$= \begin{bmatrix} c\Psi & -s\Psi & 0 \\ s\Psi & c\Psi & 0 \\ 0 & 0 & 1 \end{bmatrix} \begin{bmatrix} c\theta & 0 & s\theta \\ 0 & 1 & 0 \\ -s\theta & 0 & c\theta \end{bmatrix} \begin{bmatrix} 1 & 0 & 0 \\ 0 & c\Phi & -s\Phi \\ 0 & s\Phi & c\Phi \end{bmatrix} \quad (1)$$

$$R = \begin{bmatrix} c\Psi c\theta & s\Phi s\theta c\Psi - s\Psi c\Phi & c\Phi s\theta c\Psi + s\Psi s\Phi \\ s\Psi c\theta & s\Phi s\theta s\Psi + c\Psi c\Phi & c\Phi s\theta s\Psi - s\Phi c\Psi \\ -s\theta & s\Phi c\theta & c\Phi c\theta \end{bmatrix} \quad (2)$$

Where $c = \cos$ and $s = \sin$. Ω_1 , Ω_2 and Ω_3 are the rotational speeds in the fixed frame and are expressed as a function of the rotational speeds $\dot{\Phi}, \dot{\theta}, \dot{\Psi}$ by the following relation,

$$\Omega = [\dot{\Phi} \ \dot{\theta} \ \dot{\Psi}]^T \quad (3)$$

For small angle motion, the following applies,

$$c\Phi = c\theta = c\Psi = 1 \text{ and } s\Phi = s\theta = s\Psi = 0 \quad (4)$$

For the translation speeds we have the linear speeds v_x^b , v_y^b and v_z^b in the fixed frame. The linear speeds v_x^m , v_y^m and v_z^m in the mobile frame are given by,

$$v = \begin{bmatrix} v_x^b \\ v_y^b \\ v_z^b \end{bmatrix} = R \times \begin{bmatrix} v_x^m \\ v_y^m \\ v_z^m \end{bmatrix} \quad (5)$$

3. Physical effects on octocopter

The weight of the octocopter is given by,

$$P = mg \quad (6)$$

Where m is the total mass and g is the gravity. The lift forces are caused by the rotation of the motors. They are perpendicular to the plane of the propellers. These forces are proportional to the square of the rotational speed of the motors as follows,

$$F_i = b\omega_i^2 \quad (7)$$

Where $i = \{1:8\}$ is the index of the rotor. b is the lift coefficient [kgm/rad^2] which depends on the shape of the blades and the density of the air. The drag force is the coupling between a pressure force and the viscous friction force. The drag in the propellers is proportional to the square of the rotational speed of the rotor using,

$$T_h = d\omega_i^2 \quad (8)$$

Where d is the co-efficient of drag.

The translation on the x-axis is due to the moment created by the difference between the lift forces of the rotors 1, 2, 7, 8 and 3, 4, 5, 6 as,

$$M_y = l(F_1 + F_2 - F_3 - F_4 - F_5 - F_6 + F_7 + F_8) = lb(\omega_1^2 + \omega_2^2 - \omega_3^2 - \omega_4^2 - \omega_5^2 - \omega_6^2 + \omega_7^2 + \omega_8^2) \quad (9)$$

Where l is the length of the arm between the rotor and the center of gravity of the octocopter. The translation on the y axis is due to the moment created by the difference between the lift forces of the rotors 1, 2, 3, 4 and 5, 6, 7, 8. This moment is given by the following relation,

$$M_x = l(F_1 + F_2 + F_3 + F_4 - F_5 - F_6 - F_7 - F_8) = lb(\omega_1^2 + \omega_2^2 + \omega_3^2 + \omega_4^2 - \omega_5^2 - \omega_6^2 - \omega_7^2 - \omega_8^2) \quad (10)$$

The rotation around the z axis is due to the reactive torque caused by the pairs trained in each rotor. This moment is given by the following relation,

$$M_z = d(\omega_1^2 + \omega_2^2 - \omega_3^2 - \omega_4^2 + \omega_5^2 + \omega_6^2 - \omega_7^2 - \omega_8^2) \quad (11)$$

The pivoting of the rotors with a certain angle gives rise to gyroscopic torques which is the vector product of the kinetic moments of the rotors and of the swing speed vectors. During a rotation around y, the gyroscopic torque on the x axis is given by,

$$M_{xg} = J_{rot}\Omega_y(\omega_1^2 + \omega_2^2 - \omega_3^2 - \omega_4^2 + \omega_5^2 + \omega_6^2 - \omega_7^2 - \omega_8^2) \quad (12)$$

Similarly, the gyroscopic torque on the y axis during a rotation around x axis is given by,

$$M_{yg} = J_{rot}\Omega_x(-\omega_1^2 - \omega_2^2 + \omega_3^2 + \omega_4^2 - \omega_5^2 - \omega_6^2 + \omega_7^2 + \omega_8^2) \quad (13)$$

4. Euler-Lagrange model

Based on the calculation of variation of the Euler-Lagrange system, the generalized co-ordinates are determined the development of the rotational dynamics of the octocopter as follows,

$$q = (\Phi, \theta, \Psi) \quad (14)$$

Where Φ , θ and Ψ are the Euler angles which represent the octocopter orientation in the moving frame B. The difference between the kinetic energy T (caused by the angular velocities and the linear translation velocities) and the potential energy V denotes the Lagrangian using,

$$L = T - V \quad (15)$$

The kinetic energy of the octocopter is expressed using,

$$T = \frac{1}{2}I_x(\dot{\Phi} - \Psi \sin(\theta))^2 + \frac{1}{2}I_y(\dot{\theta} \cos(\Phi) + \Psi \sin(\Phi) \cos(\theta))^2 + \frac{1}{2}I_z(\dot{\theta} \sin(\Phi) - \Psi \cos(\Phi) \cos(\theta))^2 \quad (16)$$

The potential energy in the fixed reference is given by,

$$V = g \int x dm. (-g \sin(\theta)) + \int y dm. (g \sin(\Phi) \cos(\theta)) + \int z dm. (g \cos(\Phi) \cos(\theta)) \quad (17)$$

The Euler-Lagrange equation becomes.

$$\Gamma_i = \frac{d}{dt} \left(\frac{\partial L}{\partial \dot{q}_i} \right) - \left(\frac{\partial L}{\partial q_i} \right) \quad (18)$$

Where Γ_i is the extreme force and q_i ($i = \Phi, \theta, \Psi$) is the generalized co-ordinates.

For roll, pitch and yaw the equations are given by,

$$\frac{d}{dt} \left(\frac{\partial L}{\partial \Phi} \right) - \frac{\partial L}{\partial \Phi} = I_x \omega_x - (I_y - I_z) \omega_y \omega_z + y dm(y) \cdot (-g \cos \Phi \cos \theta) + \int z dm(z) \cdot (g \sin \Phi \cos \theta) \quad (19)$$

$$\frac{d}{dt} \left(\frac{\partial L}{\partial \theta} \right) - \frac{\partial L}{\partial \theta} = -\sin \Phi (\omega_x I_z - \omega_x \omega_y I_x - I_y) + \cos \Phi (\omega_y I_y - \omega_x \omega_z (I_z - I_x)) + \int x dm(x) \cdot (-g \cos \theta) - \int y dm(y) \cdot (g \sin \Phi \sin \theta) - \int z dm(z) \cdot (-g \cos \Phi \sin \theta) \quad (20)$$

$$\frac{d}{dt} \left(\frac{\partial L}{\partial \Psi} \right) - \frac{\partial L}{\partial \Psi} = -\sin \theta (\omega_x I_x - \omega_y \omega_z (I_y - I_z)) + \sin \Phi \cos \theta (\omega_y I_y - \omega_x \omega_z (I_x - I_z)) + \cos \Phi \cos \theta (\omega_z I_z - \omega_x \omega_y (I_x - I_y)) \quad (21)$$

Considering the hypothesis of small angles with the velocities of the Euler angles ($\Phi; \theta; \Psi$) are identical to the angular velocities in the moving reference frame $\omega_x, \omega_y, \omega_z$, the equations of motion become,

$$\begin{aligned} \Gamma_\Phi &= I_x \omega_x + (I_z - I_y) \omega_y \omega_z \\ \Gamma_\theta &= I_y \omega_y + (I_x - I_z) \omega_x \omega_z \\ \Gamma_\Psi &= I_z \omega_z + (I_y - I_x) \omega_x \omega_y \end{aligned} \quad (22)$$

By isolating the accelerations and with small angle assumptions, we obtain,

$$\begin{aligned} \ddot{\Phi} I_x &= J_{rotor} \dot{\theta} (\omega_1^2 + \omega_2^2 + \omega_5^2 + \omega_6^2 - \omega_3^2 - \omega_4^2 - \omega_7^2 - \omega_8^2) \\ &\quad + (I_y - I_z) \dot{\theta} \dot{\Psi} + bl(\omega_1^2 + \omega_2^2 + \omega_3^2 + \omega_4^2 - \omega_5^2 - \omega_6^2 - \omega_7^2 - \omega_8^2) \\ \ddot{\theta} I_y &= J_{rotor} \dot{\Phi} (-\omega_1^2 - \omega_2^2 - \omega_5^2 - \omega_6^2 + \omega_3^2 + \omega_4^2 + \omega_7^2 + \omega_8^2) \\ &\quad + (I_z - I_x) \dot{\Phi} \dot{\Psi} \\ \ddot{\Psi} I_z &= d(\omega_1^2 + \omega_2^2 - \omega_3^2 - \omega_4^2 + \omega_5^2 + \omega_6^2 - \omega_7^2 - \omega_8^2) + (I_x - I_y) \dot{\theta} \dot{\Phi} \end{aligned} \quad (23)$$

5. Newton-Euler model

The following Newton-Euler equation is used to describe the dynamics of translation,

$$m \vec{a} = \vec{P} + \sum_i \vec{F}_i \quad (24)$$

Where \vec{P} is the weight and $\sum_i \vec{F}_i$ represents the sum of the bearing capacities. By using the lift assumptions,

$$\begin{aligned} \sum_i \vec{F}_i &= b(\Omega_1^2 + \Omega_2^2 + \Omega_3^2 + \Omega_4^2 + \Omega_5^2 + \Omega_6^2 + \Omega_7^2 + \Omega_8^2) \vec{z} = \sum_i (F_i, \vec{z}) \end{aligned} \quad (25)$$

Then Eqn. (24) becomes,

$$\begin{aligned} m \begin{pmatrix} \ddot{X} \\ \ddot{Y} \\ \ddot{Z} \end{pmatrix}_{(\bar{x} \ \bar{y} \ \bar{z})} &= mg \begin{pmatrix} 0 \\ 0 \\ -1 \end{pmatrix}_{(\bar{x} \ \bar{y} \ \bar{z})} \\ + \sum_i \vec{F}_i &\begin{pmatrix} c(\Psi)s(\theta)c(\Phi) + s(\Psi)s(\Phi) \\ s(\Psi)s(\theta)c(\Phi) - c(\Psi)s(\Phi) \\ c(\theta)c(\Phi) \end{pmatrix}_{(\bar{x} \ \bar{y} \ \bar{z})} \end{aligned} \quad (26)$$

This dynamic model is adopted by several authors [2-5]. The translation model is obtained as follows,

$$\begin{aligned} \ddot{X} &= \frac{(\cos \Psi \sin \theta \cos \Phi + \sin \Psi \sin \Phi)}{m} \sum_i F_i \\ \ddot{Y} &= \frac{(\sin \Psi \sin \theta \cos \Phi - \cos \Psi \sin \Phi)}{m} \sum_i F_i \\ \ddot{Z} &= -g + \frac{(\cos \theta \cos \Phi)}{m} \sum_i F_i \end{aligned} \quad (27)$$

The complete system dynamic model according to Euler-Lagrange and Newton-Euler models for the octocopter is given by the following equations,

$$\begin{aligned} \ddot{\Psi} I_z &= d(\omega_1^2 + \omega_2^2 - \omega_3^2 - \omega_4^2 + \omega_5^2 + \omega_6^2 - \omega_7^2 - \omega_8^2) \\ &\quad + (I_x - I_y) \dot{\theta} \dot{\Phi} \end{aligned}$$

$$\ddot{Y} = \frac{(\sin \Psi \sin \Phi \cos \theta - \cos \Psi \sin \Phi)}{m} \sum_i F_i$$

$$\ddot{Z} = \frac{\cos \theta \cos \Phi}{m} \sum_i F_i$$

$$\begin{aligned} \ddot{\Phi} I_x &= J_{rotor} \dot{\theta} (\omega_1^2 + \omega_2^2 + \omega_5^2 + \omega_6^2 - \omega_3^2 - \omega_4^2 - \omega_7^2 - \omega_8^2) \\ &\quad + (I_y - I_z) \dot{\theta} \dot{\Psi} + bl(\omega_1^2 + \omega_2^2 + \omega_3^2 + \omega_4^2 - \omega_5^2 - \omega_6^2 - \omega_7^2 - \omega_8^2) \end{aligned}$$

$$\begin{aligned} \ddot{\theta} I_y &= J_{rotor} \dot{\Phi} (-\omega_1^2 - \omega_2^2 - \omega_5^2 - \omega_6^2 + \omega_3^2 + \omega_4^2 + \omega_7^2 + \omega_8^2) \\ &\quad + (I_z - I_x) \dot{\Phi} \dot{\Psi} \\ &\quad + bl(-\omega_1^2 - \omega_2^2 + \omega_3^2 + \omega_4^2 + \omega_5^2 + \omega_6^2 - \omega_7^2 - \omega_8^2) \end{aligned}$$

$$\begin{aligned} \ddot{\Psi} I_z &= d(\omega_1^2 + \omega_2^2 - \omega_3^2 - \omega_4^2 + \omega_5^2 + \omega_6^2 - \omega_7^2 - \omega_8^2) \\ &\quad + (I_x - I_y) \dot{\theta} \dot{\Phi} \end{aligned} \quad (28)$$

We notice that this model presents strong nonlinearities and a great coupling between the control inputs, also between the angles because of the gyroscopic effects and between the dynamics of rotation and the dynamics of translation. Supposedly,

$$\begin{aligned} \bar{\Omega}_r &= -\omega_1^2 - \omega_2^2 + \omega_3^2 + \omega_4^2 + \omega_5^2 + \omega_6^2 \\ &\quad - \omega_7^2 - \omega_8^2 \end{aligned} \quad (29)$$

The complete dynamic model which governs the octocopter is finalised using the following equations,

$$\begin{cases} \ddot{\Phi} = \frac{(I_y - I_z)}{I_x} \dot{\theta} \dot{\Psi} - \frac{I_r}{I_x} \bar{\Omega}_r \dot{\theta} + \frac{1}{I_x} (u_5 + u_6) \\ \ddot{\theta} = \frac{(I_z - I_x)}{I_y} \dot{\Phi} \dot{\Psi} + \frac{I_r}{I_y} \bar{\Omega}_r \dot{\Phi} + \frac{1}{I_y} (u_3 + u_4) \\ \ddot{\Psi} = \frac{(I_x - I_y)}{I_z} \dot{\Phi} \dot{\theta} + \frac{1}{I_y} (u_7 + u_8) \\ \ddot{x} = \frac{1}{m} u_x (u_1 + u_2) \\ \ddot{y} = \frac{1}{m} u_y (u_1 + u_2) \\ \ddot{z} = \frac{\cos(\Phi) \cos(\theta)}{m} (u_1 + u_2) - g \end{cases} \quad (30)$$

$$\begin{cases} u_x = c\Phi c\Psi s\theta + s\Phi s\Psi \\ u_y = c\Phi s\theta s\Psi - s\Phi c\Psi \end{cases} \quad (31)$$

$$\begin{cases} \ddot{\Phi} = \frac{(I_y - I_z)}{I_x} \dot{\theta} \dot{\Psi} - \frac{I_r}{I_x} \bar{\Omega}_r \dot{\theta} + \frac{1}{I_x} (u_5 + u_6) \\ \ddot{\theta} = \frac{(I_z - I_x)}{I_y} \dot{\Phi} \dot{\Psi} + \frac{I_r}{I_y} \bar{\Omega}_r \dot{\Phi} + \frac{1}{I_y} (u_3 + u_4) \\ \ddot{\Psi} = \frac{(I_x - I_y)}{I_z} \dot{\Phi} \dot{\theta} + \frac{1}{I_y} (u_7 + u_8) \\ \ddot{x} = \frac{1}{m} u_x (u_1 + u_2) \\ \ddot{y} = \frac{1}{m} u_y (u_1 + u_2) \\ \ddot{z} = \frac{\cos(\Phi) \cos(\theta)}{m} (u_1 + u_2) - g \end{cases} \quad (32)$$

6. PID controller

The proportional, integral, derivative (PID) controller allows performing a closed-loop control of an industrial system or process. From the trial and error method, we can establish the adjustment coefficients (P-gain, I-gain and D-gain). The measurement of system parameters is

carried out regularly at a certain sampling frequency for a given command as,

$$\text{Command} = \text{P-gain} * \text{error} + \text{I-gain} * \text{sum errors} + \text{D-gain} * (\text{error} - \text{former error}) \quad (33)$$

To set the coefficients first, a simple proportional regulator must be set up (the coefficients I-gain and D-gain are therefore zero). By trial and error, the P-gain coefficient must be adjusted in order to improve the response time of the system. In other words, a P-gain must be found which allows the system to get very close to the set-point while being cautious to keep the system stable. Once this coefficient is adjusted, we can pass to the coefficient I-gain which will cancel the final error of the system. In order for the latter to be exactly compliant with the set point, it is necessary to set I-gain to have an exact response in a short time while trying to minimize the oscillations brought by the integrator. Finally, we can pass to the coefficient D-gain which makes the system more stable. Its adjustment allows reducing oscillations.

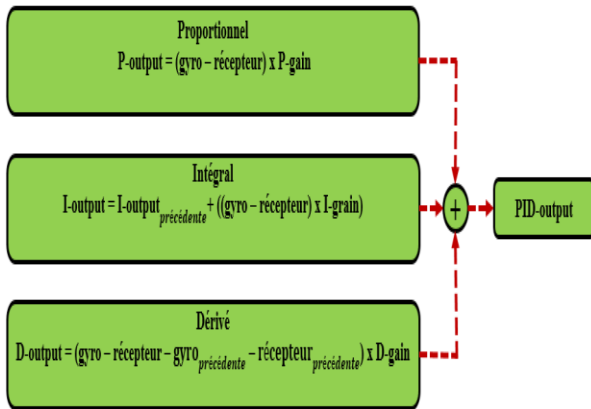


Fig. 2: Descriptive diagram of the equations used in the PID

7. Octocopter prototype

The essential components for the octocopter prototype are illustrated in Fig. 3. The micro controller handles all the necessary data and calculations. Various elements constituting the micro controller is shown in Fig. 4. Fig. 5 presents the management of the incoming and outgoing component commands for the micro controller. The realised prototype is shown in Fig. 6.

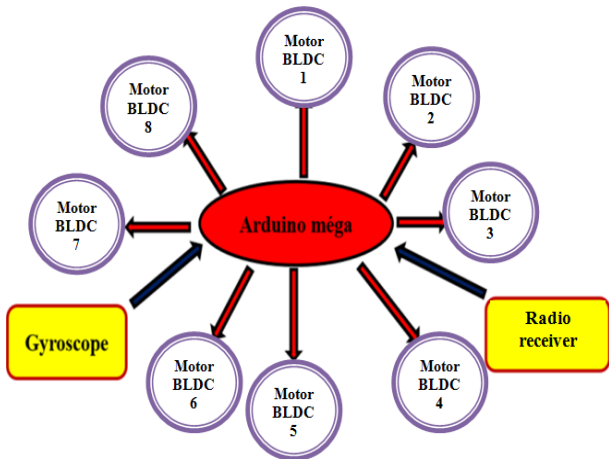


Fig. 3: Diagram of the octocopter components

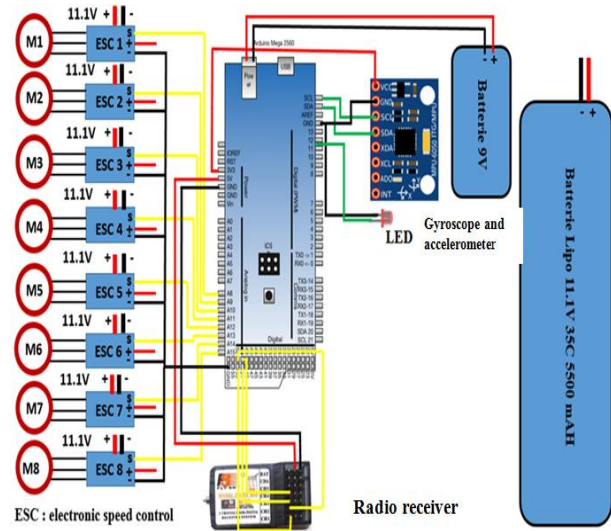


Fig. 4: Electronic schema for the micro controller

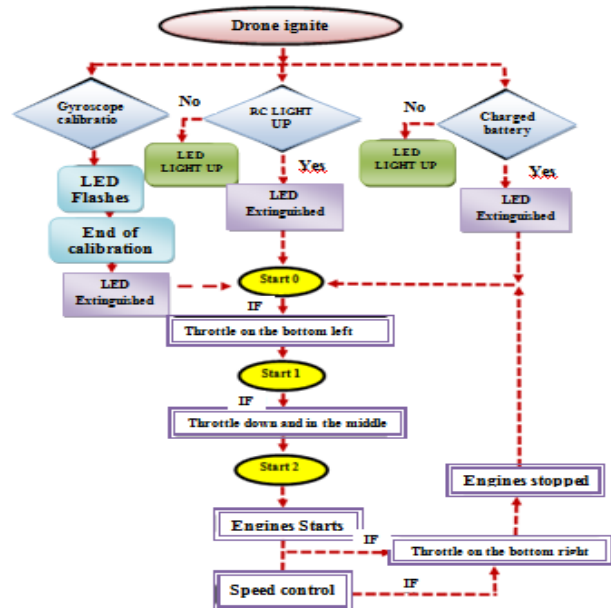


Fig. 5: Flowchart for the command



Fig. 6: Realized octocopter prototype

8. Conclusion

In order to become familiar with recent technologies and with the growth of UAV interest, we have designed and developed a prototype of octocopter for the purpose of obtaining a Master degree in Electrical Engineering. We

have met few problems during our project; one amongst them was related to the non-synchronization of the drivers. To resolve this, we had to calibrate and modify our program sequences. Despite this, we always have experienced a small margin of non-synchronization that could not be eliminated. The PID controller with the trial and error method took longer in its calculations. However, it ensured the errors made on the mechanical structure, weight distribution and balancing under wind turbulent effects.

REFERENCES:

- [1] *Les Drones Functioning, Telepilotage, Applications, Reglimentation*. 2016. 2nd Edition, New regulation, Rodolphe Jobard.
- [2] Y.Z. Boudjelthia and I. Settouti. 2013. *Modeling and Control of a Four-rotor in Six Degrees of Freedom*, Master Thesis, University Hassiba Benbouali of Chlef.
- [3] B. Musabyimana and B. Bouheraoua. 2016. *Control of Systems by a PID Corrector of Fractional Order Application: Quadri-rotor Control*, Master Thesis, Hassiba Benbouali University of Chlef.
- [4] H. Khebach. 2012. *Fault Tolerance via the Back Stepping Method of Nonlinear Systems, Application: Quadrirotor type UAV system*, Master Thesis, University Ferhat Abbas de Setif.
- [5] R. Ayad. 2010. *Design and Construction of a Quadrirotor Drone*, Master Thesis, University of Sci. and Tech. Mh. Boudiaf d'Oran.